

Dusty star forming galaxies at high redshift

A. J. Barger*, L. L. Cowie*, D. B. Sanders*, E. Fulton*, Y. Taniguchi[†], Y. Sato[†], K. Kawara[‡], & H. Okuda[§]

* Institute for Astronomy, University of Hawaii, 2680 Woodlawn Drive, Honolulu, HI 96822

[†] Astronomical Institute, Tohoku University, Aoba, Sendai 980-77, Japan

[‡] Institute of Astronomy, University of Tokyo, 2-21-1 Osawa, Mitaka, Tokyo 181, Japan

[§] Institute of Space and Astronautical Science, Yoshinodai, Sagami-hara, Kanagawa 229, Japan

The global star formation rate in high redshift galaxies, based on optical surveys, shows a strong peak at a redshift of $z \sim 1.5$, which implies that we have already seen most of the formation. High redshift galaxies may, however, emit most of their energy at submillimeter wavelengths if they contain substantial amounts of dust. The dust would absorb the starlight and reradiate it as far-infrared light, which would be redshifted to the submillimeter range. Here we report a deep survey of two blank regions of sky performed at submillimeter wavelengths (450 and 850 μm). If the sources we detect in the 850 μm band are powered by star formation, then each must be converting more than 100 solar masses of gas per year into stars, which is larger than the maximum star formation rates inferred for most optically-selected galaxies. The total amount of high redshift star formation is essentially fixed by the level of background light, but where the peak occurs in redshift for the submillimeter is not yet established. However, the background light contribution from only the sources detected at 850 μm is already comparable to that from the optically-selected sources. Establishing the main epoch of star formation will therefore require a combination of optical and submillimeter studies.

In recent years high redshift optical galaxy searches have become increasingly successful at uncovering significant populations of galaxies that are likely to be in early phases of evolution. However, the global star formation rate (SFR) inferred^{1,3,4} omits the many fainter sources that are now being detected.^{5,6} Furthermore, the effects of dust can cause the SFRs in the detected UV-bright objects to be grossly underestimated (see, e.g., ref. 7), and many rapid star forming galaxies may even be omitted from the optical samples.

Nearby star forming galaxies emit a large fraction of their bolometric luminosity in the far infrared waveband, which for distant sources is redshifted into the submillimeter waveband. Because the spectra of these star forming galaxies are very steep, if they are at large redshifts their flux density decreases much less rapidly with increasing redshift

than is expected according to the inverse square law. Thus, galaxies at high redshifts are likely to make a substantial contribution to the submillimeter counts.⁸ In a pioneering paper,⁹ Smail et al. reported the detections of submillimeter sources in the fields of two rich clusters of galaxies using the new SCUBA bolometer array¹⁰ on the 15-meter James Clerk Maxwell Telescope. These clusters were selected because they are strong gravitational lenses which magnify any submillimeter sources lying behind them. The objects in the A370 field include one spectacular source, SMM 02399–136, with an $850\mu\text{m}$ flux of 26 mJy ($1 \text{ Jy} = 1.0 \times 10^{-23} \text{ erg s}^{-1} \text{ cm}^{-2} \text{ Hz}^{-1}$). This source has subsequently been shown¹¹ to be an AGN embedded in a starburst at $z = 2.8$. Gravitational lensing greatly improves source detectability but entails an uncertain correction to remove the estimated magnification of the sources. The most likely amplification factor for the above source was given¹¹ as 2.5 with a firm upper limit of 5. The magnification problem can be avoided if blank field observations are made with longer exposure times. That is the nature of the experiment reported here and in other upcoming blank field survey papers by UK and UK-Canadian teams.

We obtained SCUBA observations of two blank field areas, one in the Lockman hole and one in the Hawaii deep field region SSA13. Our data were taken during 8 eight-hour shifts in March 1998 and 8 eight-hour shifts in May 1998. Fully sampled wavelength maps were completed simultaneously in both the long ($850\mu\text{m}$) and short ($450\mu\text{m}$) wavelength arrays, but the sky at $450\mu\text{m}$ is considerably more opaque. Although two of the 16 shifts were too poor to contribute significantly to the observations, much of the run had superb weather conditions and produced sensitive maps at both wavelengths. For the $850\mu\text{m}$ maps, which are of primary interest, the total integration time was 39 hours on the Lockman hole region and 51 hours on SSA13.

At $450\mu\text{m}$ no sources were detected at the 3σ level of 25 mJy in either field. At $850\mu\text{m}$ two sources having fluxes $> 3 \text{ mJy}$ were detected at the $> 3\sigma$ level, one in each field; these are listed in Table 1. The $850\mu\text{m}$ maps are described and shown in Figure 1. The absolute value of the noise was found from the dispersion of the points in the map, excluding the regions around the brightest sources (see Table 1). Based on predictions of source confusion,¹² the instrumental and sky noise are expected to dominate the total noise. The completeness of source recovery as a function of flux was tested using Monte Carlo simulations. Five sources at each of a range of flux levels were simulated using the beam derived from the calibration source and were added into the field. The source was considered to be recovered if it was detected at the 3σ level by the source detection algorithm. This procedure was repeated a large number of times at each flux. Recovery of sources brighter than 3 mJy was essentially complete, except for a small number of cases where the objects overlapped. The fall off in recovery was extremely rapid, with 80 per cent of the sources recovered around 3 mJy and only 20 per cent by 2 mJy. Inspection of the negative images yielded no sources with

fluxes greater than 3 mJy. Given that we detect only two sources in our data maps with fluxes above 3 mJy using the same 3σ threshold, we may conclude that the surface density of sources above 3 mJy is 800 (290–1900) deg^{-2} , where the numbers in parentheses are the $\pm 1\sigma$ range. Our number is smaller than the tentative estimate of $2500 \pm 1400 \text{ deg}^{-2}$ above 4 mJy made in ref. 9 on the basis of observations of cluster-lensed sources. This difference may partially reflect the uncertainty in the magnification correction but could also arise in large part from the small-number statistics of the observations. Our value corresponds to a νS_ν , where S_ν is the sky surface brightness, of $3.7 \times 10^{-8} \text{ ergs cm}^{-2} \text{ s}^{-1} \text{ ster}^{-1}$, which is a factor of a few less than current limits on the extragalactic background light.^{13,14,15,16,17}

Our strongest source in the two fields is the 4.6 mJy ($\sim 6\sigma$) source in the Lockman hole. In Figure 2 we show a deep K' image of the Lockman hole SCUBA field with a 3 mJy/beam contour superimposed on the bright source. We also show deep zoomed K' and B -band images of the region surrounding the source. An optical spectrum obtained with the Low Resolution Imaging Spectrometer (LRIS¹⁸) on the Keck 10-meter telescope reveals only continuum emission. Since [OII] 3727Å would shift out of the observed spectral range for $z \gtrsim 1.5$, this suggests that the source lies above this redshift limit. However, the presence of the object in the B -band image places an upper limit on the redshift of the source of $z \lesssim 3.5$.

Given these redshift constraints, the only class of local objects whose spectral energy distribution (SED) could provide an approximate match to the K' and 850 μm flux measurements of our brightest source is an ultraluminous infrared galaxy.¹⁹ For the following discussion we assume that the SED of the “prototypical” ultraluminous infrared galaxy Arp 220 is appropriate for our object. The spectral shape of Arp 220 can be represented²⁰ by a modified blackbody with emissivity λ^{-1} and a dust temperature of $T = 47 \text{ K}$. If we place an Arp 220 source at a redshift z , the effective blackbody temperature becomes $T/(1+z)$ due to the expansion of the Universe. The far infrared luminosity (L_{FIR}) can then be related to the observed 850 μm flux of our brightest source. Assuming the Arp 220 temperature of $T = 47 \text{ K}$, we find $L_{\text{FIR}} = (0.9 - 1.6) \times 10^{12} L_\odot h_{75}^{-2}$ for $q_0 = 0.5$ and $(1.2 - 6.1) \times 10^{12} L_\odot h_{75}^{-2}$ for $q_0 = 0.02$ over the redshift range $0.5 < z < 3.5$. Submillimeter observations of nearly all luminous infrared galaxies have been reasonably fit by single temperature dust models¹⁹ with $T = 30 - 50 \text{ K}$; thus, the temperature dependence of L_{FIR} introduces a factor of only about 0.2–1.2 uncertainty in the above L_{FIR} numbers.

Although we do not have radio spectral indices or diagnostic spectral line ratios that are traditionally used to discriminate between thermal and non-thermal energy sources, it is probable, as in the low- z ultraluminous infrared galaxies, that the energy in our submillimeter sources is powered by a mixture of AGN and star formation with a substantial fraction arising from the star formation. If we assume that all of the energy originally in the rest

frame ultraviolet is reradiated into the FIR and take the extreme case of zero contribution to the FIR emission from an obscured AGN, then the FIR luminosity provides a measure of the current SFR of massive stars^{21,22} $\text{SFR} = \Psi 10^{-10} (L_{\text{FIR}}/ L_{\odot}) M_{\odot} \text{ yr}^{-1}$, where $\Psi = 0.8 - 2.1$. To produce all of the luminous energy of our brightest source from intense ongoing star formation would therefore require star formation rates of $(140 - 250) M_{\odot} \text{ yr}^{-1} h_{75}^{-2}$ for $q_0 = 0.5$ and $(180 - 910) M_{\odot} \text{ yr}^{-1} h_{75}^{-2}$ for $q_0 = 0.02$, taking $\Psi = 1.5$. This is an order of magnitude higher than the star formation rates typically seen in rapidly star forming galaxies observed in the optical^{2,3} and is similar to rates predicted from other recent submillimeter observations (see, e.g., ref. 23). Thus, our data indicate that the upper end of the mass formation function is dominated by objects that are radiating primarily in the submillimeter.

The relative fraction of the universal stellar energy which is reradiated into the submillimeter and is present in these bright submillimeter sources versus that which is radiated in the rest frame ultraviolet is most simply quantified using the extragalactic background light. If we assume an Arp 220 spectrum for the submillimeter objects and a substantial fraction of light powered by star formation, then the sum of our two measured $> 3\sigma$ $850\mu\text{m}$ source fluxes, if located at $z = 1$, would require reradiation of a rest frame ultraviolet sky brightness of $S_{\nu} = 9 \times 10^{-25} \text{ ergs cm}^{-2} \text{ s}^{-1} \text{ Hz}^{-1} \text{ deg}^{-2}$ to produce the bolometric submillimeter light. [The redshift dependence of S_{ν} is approximately $((1+z)/2)^{-2.3}$]. In comparison, the integrated flat spectrum population corresponding to the peak of the optically selected star forming galaxies near $z = 1$ gives a rest frame ultraviolet surface brightness²⁴ of approximately $4 \times 10^{-25} \text{ ergs cm}^{-2} \text{ s}^{-1} \text{ Hz}^{-1} \text{ deg}^{-2}$. While the submillimeter results are still quite uncertain due to the small number of sources, these two values are quite comparable, with the submillimeter light from the bright sources dominating if they lie at $z \lesssim 1.7$. More accurate estimates will require the observations of many SCUBA fields to the level described here.

In summary, our results suggest that high redshift star forming galaxies with the largest star formation rates radiate primarily in the submillimeter. Further support for this argument has been obtained in very recent cluster observations.²⁵ Although these submillimeter sources with high star formation rates are less common than are optically-selected galaxies, the integrated light emitted by the submillimeter sources and by the optically-selected galaxies appears to be comparable within the still considerable uncertainties in the surface densities. The present results probe only the highest luminosity submillimeter sources, and recent measurements of the integrated backgrounds indicate that several times more energy could be present in fainter submillimeter sources.^{13, 14, 15, 16, 17}

REFERENCES

1. Madau, P. et al. High-redshift galaxies in the Hubble Deep Field: colour selection and star formation history to $z \sim 4$. *Mon. Not. R. Astr. Soc.* **283**, 1388–1404 (1996)
2. Pettini, M. et al. The discovery of primeval galaxies and the epoch of galaxy formation, in Cosmic origins: evolution of galaxies, stars, planets, and life, eds. Shull, J. M., Woodward, E. E., & Thronson, H. A., *Astr. Soc. Pac.*, **in press**, [astro-ph/9708117](#) (1998)
3. Steidel, C. C., Giavalisco, M., Pettini, M., Dickinson, M., & Adelberger, K. L. Spectroscopic confirmation of a population of normal star-forming galaxies at redshifts $z > 3$. *Astrophys. J.* **462**, L17–L21 (1996)
4. Cowie, L. L., Hu, E. M., Songaila, A., Egami, E. The evolution of the distribution of star formation rates in galaxies. *Astrophys. J.* **481**, 9 (1997)
5. Cowie, L. L. & Hu, E. M. High- z Lyman-alpha emitters. I. a blank-field search for objects near redshift $z = 3.4$ in and around the Hubble Deep Field and the Hawaii Deep Field SSA22. *Ast. J.* **115**, 1319–1328 (1998)
6. Hu, E. M., Cowie, L. L., & McMahon, R. G. The density of Lyman-alpha emitters at very high redshift. *Astrophys. J.* **in press**, [astro-ph/9803011](#) (1998)
7. Heckman, T. M., Robert, C., Leitherer, C., Garnett, D. R., & van der Rydt, F. The ultraviolet spectroscopic properties of local starbursts: implications at high-redshift. *Astrophys. J.* **in press**, [astro-ph/9803185](#) (1998)
8. Blain, A. W. & Longair, M. S. Submillimeter cosmology. *Mon. Not. R. Astr. Soc.* **264**, 509 (1993)
9. Smail, I., Ivison, R. J. & Blain, A. W. A deep submillimeter survey of lensing clusters: a new window on galaxy formation and evolution. *Astrophys. J.* **490**, L5–L8 (1997)
10. Holland, W. S. et al. SCUBA – a submillimeter camera operating on the James Clerk Maxwell Telescope, in Advanced technology MMW, radio and terahertz telescopes, ed. Phillips, T., *Proc. SPIE* **3357**, **in press** (1998)
11. Ivison, R. J. et al. A hyperluminous galaxy at $z = 2.8$ found in a deep submillimeter survey. *Mon. Not. R. Astr. Soc.* **in press**, [astro-ph/9712161](#) (1998)
12. Blain, A. W., Ivison, R. J., & Smail, I. Observational limits to source confusion in the millimeter/submillimeter waveband. *Mon. Not. R. Astr. Soc.* **296**, L29–33 (1998)

13. Puget, J. L. et al. Tentative detection of a cosmic far infrared background with COBE. *Astr. Astrophys.* **308**, L5–L8 (1996)
14. Burigana, C. et al. Constraints on the cosmic star formation history from the far-infrared background. *Mon. Not. R. Astr. Soc.* **287**, L17–L20 (1997)
15. Fixsen, D. J., Dwek, E., Mather, J. C., Bennett, C. L., & Shafer, R. A. The spectrum of the extragalactic far infrared background from the COBE firas observations. *Astrophys. J.* **in press**, **astro-ph/9803021** (1998)
16. Schlegel, D., Finkbeiner, & D. P., Davis, M. Maps of dust IR emission for use in estimation of reddening and CMBR foregrounds. *Astrophys. J.* **500**, 525 (1998)
17. Hauser, M. G. et al. The COBE diffuse infrared background experiment search for the cosmic infrared background: I. limits and detections. *Astrophys. J.* **in press**, **astro-ph/9806167** (1998)
18. Oke et al. The Keck low-resolution imaging spectrometer. *Pub. Ast. Soc. Pac.* **107**, 375-385 (1995)
19. Sanders, D. B. & Mirabel, I. F. Luminous infrared galaxies. *A. Rev. Ast. Astrophys.* **34**, 749-782 (1996)
20. Klaas, U., Haas, M., Heinrichsen, I. & Schulz, B. Infrared spectral energy distributions of the interacting galaxies Arp 244, NGC 6240, and Arp 220. *Astr. Astrophys.* **325**, L21-L24 (1997)
21. Scoville, N. Z. & Young, J. S. The molecular gas distribution in M51. *Astrophys. J.* **265**, 148 (1983)
22. Thronson, H. & Telesco, C. Star formation in active dwarf galaxies. *Astrophys. J.* **311**, 98 (1986)
23. Cimatti, A., Andreani, P., Röttgering, H., & Tilanus, R. Vigorous star formation hidden by dust in a galaxy at $z = 1.4$. *Nature* **392**, 895–896 (1998)
24. Songaila, A., Cowie, L. L., & Lilly, S. J. Galaxy formation and the origin of the ionizing flux at large redshift. *Astrophys. J.* **348** 371-377 (1990)
25. Blain, A. W., Smail, I., Ivison, R. J., & Kneib, J.-P. The history of star formation in dusty galaxies. *Mon. Not. R. Astr. Soc.* **submitted**, **astro-ph/9806062** (1998)
26. Jenness, T. SURF – SCUBA user reduction facility. *Starlink User Note* **216.1** (1997)

27. Hodapp, K.-W. et al./ The HAWAII infrared detector arrays: testing and astronomical characterization of prototype and science-grade devices. *New Astronomy* **1**, 177-196 (1996)
28. Matthews, K. & Soifer, B. T. The Near Infrared Camera on the W. M. Keck Telescope, in *Infrared astronomy with arrays: the next generation*, ed. McLean, I. (Dordrecht: Kluwer), 239-246 (1994)

We are grateful to Remo Tilanus, Tim Jenness, Ian Smail, and William Vacca for valuable interactions. We thank the two referees and the editor for comments which led to substantial improvements in the paper.

FIGURES

Figure 1 850 μ m SCUBA maps of our two blank fields: (left) Lockman Hole and (right) SSA13. The top panels show the total integrations, the middle panels show just the data from our May 1998 run, and the bottom panels show just the data from our March 1998 run. The vertical maps have their centers aligned. The field centers for the Lockman Hole are RA(2000) 10 33 55.4 and Dec(2000) 57 46 18 and for SSA13 are RA(2000) 13 12 25.6 and Dec(2000) 42 44 38. The diameter of each of the maps is ~ 2.7 arcmin. The exposure times for the maps are (a) 38.8 hrs, (b) 8.1 hrs, (c) 30.7 hrs, (d) 51.0 hrs, (e) 34.8 hrs, and (f) 16.2 hrs. The contours show levels of constant surface brightness. In the central regions of the Lockman Hole maps the first contour level is 2.2 mJy or $\sim 3\sigma$, and the second contour level is 4.4 mJy or $\sim 6\sigma$. In the central regions of the SSA13 maps the contour level is 2.2 mJy or $\sim 3\sigma$. Any features right at the edges of the maps are insignificant at even the 1.5σ level due to the rapid increase in the noise levels at the very edge. Therefore, the only feature in the total maps other than the two sources listed in Table 1 that we feel might be real is the 2.5 mJy feature approximately 45 arcsec north of the identified source in the SSA13 map. The SCUBA observations were obtained by stepping the secondary mirror through a 64-point jiggle pattern in Nasmyth coordinates while chopping at a frequency of 6.94 Hz and a chop throw of 45 arcsec in RA. In order to cancel out the sky, the jiggle pattern was subdivided and the target position switched between the signal and reference beams using a repeating signal-reference-reference-signal scheme. Because the chop throw is small the reference negative images also appear on the array and hence can be restored, increasing the effective exposure times on most of the field. The primary source extraction was done using beam- and exposure-weighting to determine the signal and noise at each spatial position, and both positive and negative portions of the beam pattern were used. Pointing checks were performed every hour using the blazars 0923+392 or 1308+326, and our data maps were calibrated using twice-nightly beam maps of the calibration source CRL618 (March run) or thrice-nightly beam maps of IRC+10216 (May run). The measurement of the calibration source was found to vary by a maximum of ~ 20 per cent over the course of a shift. “Skydips”, which measure the zenith atmospheric opacities at 450 and 850 μ m, were done every few hours throughout each night, and the sky opacity at 230 GHz was monitored at all times to keep track of the stability of the sky. The data were reduced in a standard way using the dedicated SCUBA data reduction software SURF.²⁶

Figure 2 (a) 3 mJy/beam contour of the $\sim 6\sigma$ source detected in the 850 μ m Lockman hole map displayed on a K' image obtained with the QUick Infrared Camera (QUIRC²⁷) on the University of Hawaii 88-inch telescope on Mauna Kea during the period of 1995-1996. The units on the axes are arcseconds, and the square box is the zoomed region shown in (b). (b) Zoomed K' image of the source (field center) obtained with the Near Infrared Camera

(NIRC²⁸) on the Keck 10-m telescope in March 1998; $K'_{AB} = 21.8$. The displayed field is ~ 45 arcsec on a side. (c) Zoomed B image obtained with the University of Hawaii 88-inch telescope in March 1998; $B_{AB} = 23.5$. The displayed field is ~ 45 arcsec on a side. Magnitudes were measured in 6 arcsec diameter apertures and put into the AB magnitude system [$AB = -2.5 \log f_\nu - 48.60$, where f_ν is the flux in $\text{ergs cm}^{-2} \text{ s}^{-1} \text{ Hz}^{-1}$].

Table 1. 850 μ m Sources

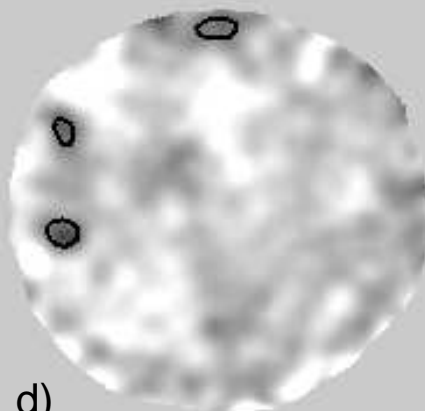
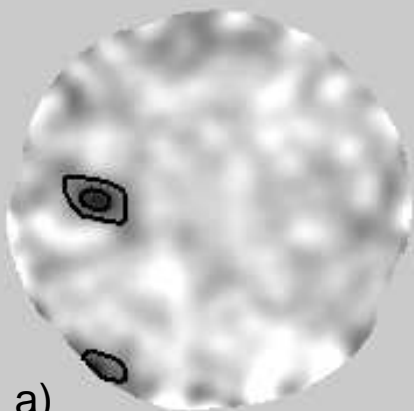
Field	RA(2000)	Dec(2000)	Flux (mJy)	1σ noise level at source position (mJy)
Lockman hole	10 34 02.3	57 46 25.0	4.6	0.8
SSA13	13 12 32.1	42 44 28.0	3.3	0.9

Note. — The UT 1998 dates and zenith 850 μ m sky optical depth ranges for the March run were 17 (0.30 – 0.31), 19 (0.42 – 0.47), 20 (0.20 – 0.35), 21 (0.13 – 0.14), 22 (0.13 – 0.30), 23 (0.13 – 0.24), 24 (0.10 – 0.11), 25 (0.10) and for the May run were 16 (0.28 – 0.41), 17 (0.27 – 0.36), 18 (0.28 – 0.38), 19 (0.45 – 0.58), 22 (0.11 – 0.14), 23 (0.11 – 0.14), 24 (0.20 – 0.23), and 25 (0.16 – 0.25). During the March run the airmass range for the Lockman Hole was 1.3 – 2.4 and for SSA13, 1.1 – 1.4. For the May run the airmass range for the Lockman Hole was 1.3 – 1.5 and for SSA13, 1.1 – 1.7.

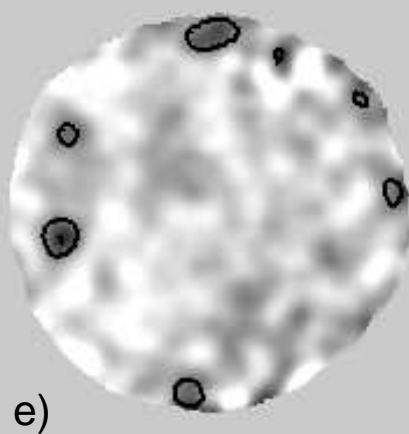
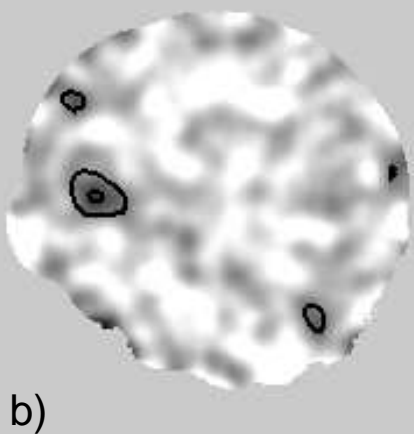
LOCKMAN

SSA13

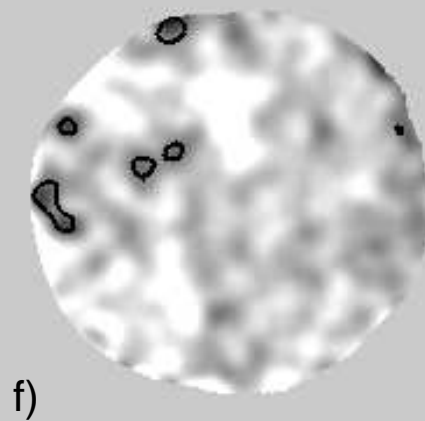
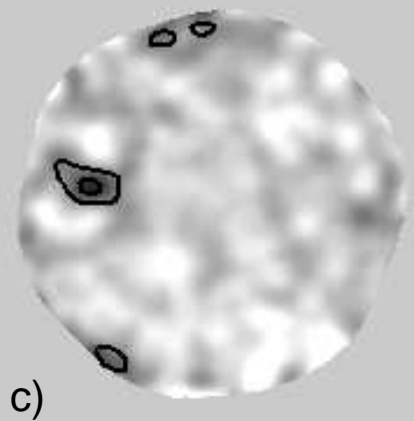
850 μm



TOTAL



May 98



March 98

